Environmental Science & Technology

pubs.acs.org/est

Article

Improved Settling Velocity for Microplastic Fibers: A New Shape-Dependent Drag Model

Jiaqi Zhang and Clarence Edward Choi*

Cite This: https://doi.org/10.1021/acs.est.1c06188

Read Online

ACCESS | Metrics & More | Article Recommendations | Supporting Information

ABSTRACT: Microplastics are abundant in aquatic environments and are an emerging environmental concern. The prediction of their settling velocities is central to predictions of the residence time and concentration depth profiles of microplastics in aquatic environments. The main scientific challenge in improving the current understanding of the settling motions of microplastics is that existing drag models are deficient at reasonably predicting the settling velocities of various microplastics, especially microplastic fibers. This is because the shape factors used in the existing drag models cannot morphologically distinguish fibers from fragments and films. In this study, a new shape factor, specifically the Aschenbrenner shape factor, is proposed as a vehicle to explicitly distinguish among the morphologies of fibers, films, and fragments. With this new shape factor, a new drag model is developed and then systematically evaluated against the unique set of data provided by new experiments conducted in this study along with four other published data sets in the literature. The proposed model allows the prediction of the terminal settling velocity of microplastic fibers more accurately than existing drag models. Moreover, the new model has also shown its applicability to microplastic films and fragments. Notwithstanding, the new model appears deficient at reasonably predicting the terminal settling velocity of weathered microplastics in the field, which requires further investigations.

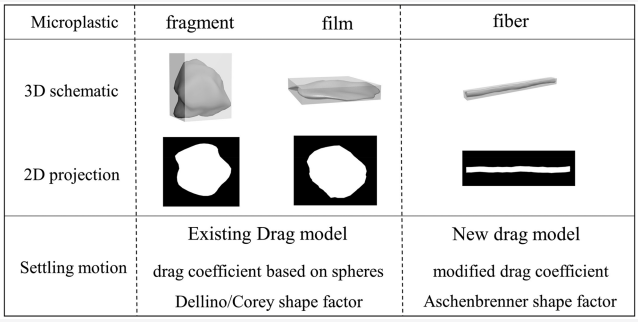

KEYWORDS: *microplastic fibers, aquatic environment, drag model, settling velocity, shape dependence*

1. INTRODUCTION

Microplastics, especially fibers, are abundant in aquatic environments and are an emerging environmental concern.[1,2] This is because high concentrations of fibers are released along with laundry effluent and discharged into aquatic environments.[3] These fibers are an environmental concern[4,5] because they have been reported to enter the food chain.[6] The existing foundation of work on microplastic fibers places a strong emphasis on pollution detection[7,8] and plastic toxicity.[9] However, there remains a dearth of literature that investigates the basic settling motion of microplastic fibers in a quiescent fluid, such as water. Although there is an increasing number of studies on measuring the terminal settling velocities of microplastic fibers in quiescent water,[10,11] analytical drag models that enable predictions of the terminal settling velocities of microplastics are far and few between.[12] The prediction of terminal settling velocities of fibers is important because it governs the residence time[10] and concentration depth profiles[11] of microplastics in water, both of which determine whether microplastics will accumulate in the food chain.[13] Moreover, predicting the terminal settling velocities of microplastic fibers is a prerequisite for numerically modeling their complex transportation,[14] sedimentation,[15,16] and entrainment[17] processes in aquatic environments. Thus, without reasonable predictions of the terminal settling velocities of microplastic fibers, progress toward the identification of the extent of microplastic pollution in aquatic environments and the development of potential remediation strategies may be hindered.[18,19]

The terminal settling velocity, u_t, of a particle with any morphology in a quiescent fluid is theoretically described as follows:[20]

$$u_t = \sqrt{\frac{2V}{A_P C_D}\frac{\rho_m - \rho_f}{\rho_f} g} \tag{1}$$

where V is the volume of the particle, A_P is the projected area of the particle in the plane orthogonal to the settling direction, C_D is the drag coefficient, ρ_m is the particle density, ρ_f is the fluid density, and g is the gravitational acceleration. The drag

Received: September 20, 2021
Accepted: November 16, 2021

Table 1. Summary of Existing Drag Models for Microplastic Fibers Settling in a Quiescent Fluid

	Khatmullina et al.[38]	Waldschlager et al.[12]	Dioguardi et al.[29]
equivalent diameter (d_{eq})[a]	longest length (D_L)	shortest length (D_S)	volume equivalent diameter (D_{eqv})
shape factor[b]	no	Corey shape factor (CSF)	Dellino shape factor (Ψ)
Reynolds number (Re)[c]	$Re = u_{t,mea} D_L/\vartheta$	$Re = u_{t,mea} D_S/\vartheta$	$Re = u_{t,mea} D_{eqv}/\vartheta$
drag model	$CD = 55.238DL + 12.691Re$	$C_D = \frac{4.7}{\sqrt{Re}} + \sqrt{CSF}$	$C_D = \frac{24}{Re}\left(\frac{1-\Psi}{Re}\right)^{0.25} + \frac{24}{Re}(0.1806Re^{0.6459})\Psi^{-Re^{0.08}} + \frac{0.4251}{1+\frac{6880.95}{Re}\Psi^{5.05}}$
calculated terminal settling velocity ($u_{t,cal}$)[d]	$u_{t,cal} = \frac{\pi}{2}\frac{1}{\nu}\frac{D_L D_S g'}{55.238D_L + 12.691}$	$u_{t,cal} = \sqrt{\frac{4}{3}\frac{D_S}{C_D}g'}$	$u_{t,cal} = \sqrt{\frac{4}{3}\frac{D_{eqv}}{C_D}g'}$

[a] D_L, D_I, and D_S are the longest, intermediate, and shortest lengths of a microplastic, respectively. D_{eqv} is the volume equivalent diameter of a microplastic. [b] Shape factors are calculated as follows:

$$CSF = \frac{D_S}{\sqrt{D_L D_I}};\ \Psi = \frac{\Phi}{\chi};\ \Phi = \frac{A_{sph}}{A_S};\ A_{sph} = 4\pi\left(\frac{D_{eqv}}{2}\right)^2;$$

$$A_S = 4\pi\left[\frac{(D_L D_I/4)^{1.6075} + (D_L D_S/4)^{1.6075} + (D_S D_I/4)^{1.6075}}{3}\right]^{1/1.6075};$$

$$\chi = \frac{P_{mp}}{P_c}$$

where ϕ is the sphericity of a microplastic particle, A_{sph} is the surface area of a sphere with the equivalent volume of the microplastic particle, A_S is the surface area of a microplastic particle, χ is the circularity of the microplastic particle, P_{mp} is the maximum projected perimeter of a microplastic particle, and P_c is the perimeter of a circle equivalent to the perimeter of the microplastic particle based on its maximum projected area. [c] $u_{t,mea}$ is the measured terminal settling velocity, and ϑ is the kinematic viscosity of the fluid. [d] g' is the corrected gravitational acceleration, which is calculated as $(\rho_m - \rho_f)g/\rho_f$ **2.**

coefficient is a dimensionless parameter that quantifies the resistance induced by a fluid on a particle.

For the drag coefficient of a spherical particle, eq 1 can be rearranged as follows:

$$C_D = \frac{4}{3}\frac{d}{u_t^2}\frac{\rho_m - \rho_f}{\rho_f}g \tag{2}$$

where u_t is the terminal settling velocity and d is the diameter of the sphere. Based on eq 2, analytical drag models have been proposed for the predictions of the terminal settling velocities of sediments with irregular morphologies.[21−23] Generally, the shape factors that are used to characterize the irregular morphology of sediments are included in the drag models.[24]

It is commonly hypothesized that the settling behavior of microplastics is similar to that of sediments.[12] Thus, most studies related to microplastics directly adopt the drag models proposed for sediments (e.g., the models of Dietrich,[21] Camenen et al.,[22] and Zhiyao et al.[23]) to predict the terminal settling velocities of microplastics. However, there has been little discussion on whether the drag models for sediments are in fact suitable for predicting the settling velocities of microplastics. Recently, Waldschlager et al.[12] and Melkebeke et al.[25] carried out pioneering work to study this problem. Waldschlager et al.[12] compared the terminal settling velocities of microplastics calculated by using six different analytical drag models[21−23,26−28] that were originally proposed for sediments with measured velocities from experiments. It was concluded that the six drag models[21−23,26−28] that were evaluated exhibited deficiencies in predicting the terminal settling velocities of microplastics, especially for fibers.[12] Subsequently, Waldschlager et al.[12] proposed the drag models for fibers and nonfibrous microplastics. Such models exhibited the lowest errors for predictions of the terminal settling velocities of microplastics compared to the six analytical drag models proposed for sediments.[21−23,26−28] Similarly, Melkebeke et al.[25] evaluated ten drag models[21,22,24,29−36] proposed for sediments. Among the evaluated models, the one proposed by Dioguardi et al.[29] was identified as the best one because it exhibited the lowest errors (i.e., 9% for fragments, 10% for films, and 37% for fibers) for predictions of the terminal settling velocities of microplastics (cf. the Supporting Information of Melkebeke et al.[25]). Thus, it can be found from the studies of Waldschlager et al.[12] and Melkebeke et al.[25] that the drag models originally proposed for sediments, which are widely used in previous studies on microplastics (i.e., the models of Dietrich,[21] Camenen et al.,[22] and Zhiyao et al.[23]), may not be entirely appropriate for predictions of the terminal settling velocities of microplastics.

Moreover, the drag models that were exclusively developed and proposed for microplastics[12] were also systematically evaluated by Melkebeke et al.[25] The average errors of the models proposed by Waldschlager et al.[12] for fragments, films, and fibers were reported to be 17%, 40%, and 62%, respectively (cf. the Supporting Information of Melkebeke et al.[25]). It can be found that both the model proposed by Dioguardi et al.[29] (i.e., deemed to exhibit the best performance for microplasticsby Melkebeke et al.[25]) and the model proposed by Waldschlager et al.,[12] which was exclusively proposed for microplastics, exhibited higher errors for the predictions of the terminal settling velocities of fibers compared to fragments and films. The higher errors for fibers compared to other morphologies should not be surprising since the shape factors used in the drag models proposed by Dioguardi et al.[29] and Waldschlager et al.[12] do not explicitly characterize the unique morphology of fibers, which is known to govern their settling velocities.[24] More specifically, the drag models proposed by

https://doi.org/10.1021/acs.est.1c06188
Environ. Sci. Technol. XXXX, XXX, XXX−XXX

Waldschlager et al.[12] and Dioguardi et al.[29] adopted the Corey shape factor (CSF) and the Dellino shape factor (Ψ), respectively. Melkebeke et al.[25] evaluated the applicability of different shape factors for charactersing the morphology of microplastic particles and reported that the Corey shape factor cannot be used to clearly distinguish between fibers and films. Moreover, the Dellino shape factor is dependent on sphericity, which gives an incomplete description of the morphology of fibers.[37] It is interesting to note that the Dellino shape factor was initially used to describe the shape of pumices, which are fragment-like in morphology and have little morphological resemblance to fibers.[32]

In addition, Khatmullina et al.[38] also proposed a drag model exclusively for microplastic fibers. While this model was not evaluated by Melkebeke et al.,[25] its accuracy and range of applicability appear limited because it even does not include a shape factor that accounts for the morphology of fibers.

Taken together, a new shape factor that can distinguish between fibrous and nonfibrous microplastics is required to improve the predictions of the terminal settling velocities of microplastic fibers. Table 1 gives a summary of the aforementioned three drag models that have been deemed suited to microplastics.[12,29,38]

Turning now to other fields, although some studies on the settling motion of fibers have been reported in the physics discipline, these studies mainly focus on the orientation and deformation of a fiber as it settles in water rather than the predictions of its terminal settling velocities.[39,40] Additionally, research work has been carried out to predict the terminal settling velocity of a single fiber settling in air.[41,42] Nonetheless, the outcomes pertaining to a fiber settling in air may have limited applicability to fibers settling in water. This is because the drag force of a fiber settling in the air is mainly governed by frictional drag.[41] In contrast, a fiber settling in water is mainly governed by pressure drag.[24] Moreover, due to the apparent density difference between air ($\sim 10^{0}$ kg/m^3) and water ($\sim 10^3$ kg/m^3), the trajectory of a fiber settling in air exhibits much greater oscillations[41] compared with of the trajectory of a fiber settling in water.[12,38] It is evident that existing studies that focus on the settling motion of fibers in other fields[39−42] may not have direct relevance for making predictions of the terminal settling velocities of microplastic fibers in aquatic environments.

The aim of this study is to improve the prediction of the terminal settling velocity of microplastic fibers. A new shape factor is identified and used to distinguish between fibrous and nonfibrous microplastics. With the newly identified shape factor, a new shape-dependent drag model for microplastic fibers is put forward. The newly proposed drag model is systematically evaluated against five independent data sets.

2. METHOD

2.1. New Shape-Dependent Drag Model. *2.1.1. Determination of Equivalent Diameter and Drag Coefficient.* For nonspherical particles, the drag coefficient can be determined by using eq 1 along with the measured terminal settling velocities if the volume (V) and projected area (A_P) of a particle are known a priori. The volume of a particle with the irregular morphology can be determined based on the measured mass and density (i.e., $V = M/\rho_m = D_{eqv}^3\pi/6$, where M is the particle mass, ρ_m is the particle density, and D_{eqv} is the measured volume equivalent diameter).[25] However, determining the projected area of particles with irregular morphologies is not straightforward.[43] Generally, in drag models, the projected area of a particle with irregular morphology is approximated by using the characteristic length of the particle (i.e., the equivalent diameter d_{eq}).[44] Consequently, before the drag coefficient can be determined, the equivalent diameter should be obtained to approximate the projected area of a microplastic particle.

According to slender body theory[45] and experimental evidence,[12,38] an elongated body (e.g., cylinder, rod, and microplastic fiber) that settles in a quiescent fluid tends to align its maximum cross-sectional area (A_{mc}) perpendicularly to the settling direction. Thus, the maximum cross-sectional area is adopted herein to characterize the projected area such that the area equivalent diameter (D_{eqa}) is treated as the equivalent diameter (d_{eq}). The maximum cross-sectional area is calculated by using the minimum bounding box method proposed by Blott et al.,[46] and the equivalent diameter is calculated as follows:

$$d_{eq} = D_{eqa} = \sqrt{4A_{mc}/\pi} = \sqrt{4D_L D_I/\pi} \tag{3}$$

where D_L and D_I are the longest and intermediate lengths of a microplastic particle, respectively.

With the calculated projected area ($A_p = \pi d_{eq}^2/4$) and the measured volume ($V = M/\rho_m = D_{eqv}^3\pi/6$), the expression for the drag coefficient of a microplastic particle with any morphology can be obtained by rearranging eq 1 as follows:

$$C_D = \frac{4}{3}\frac{D_{eqv}^3}{d_{eq}^2 u_t^2}\frac{\rho_m - \rho_f}{\rho_f}g \tag{4}$$

2.1.2. New Shape Factor. The new shape factor should be able to distinguish fibers from fragments and films not only in morphology but also in terms of hydrodynamics.[24] This is because the overall drag coefficient that accounts for the hydrodynamic resistance of a settling particle includes the contributions from the pressure drag coefficient (C_{DP}) and the frictional drag coefficient (C_{DF}):[47]

$$C_D = C_{DP} + C_{DF}\frac{A_S}{A_P} \tag{5}$$

In eq 5, the morphology of a particle can be described by using the ratio between the surface (A_s) and projected area (A_p).[48] Although this ratio provides a strong linkage between particle morphology and hydrodynamics, measuring the surface and projected area of fibers with irregular morphologies is not entirely a straightforward process. On the other hand, the maximum cross-sectional area (A_{mc}) in eq 3 can be used to approximate the projected area, however, the surface area of an entire microplastic particle cannot be described by just using the morphological information in the plane of projection. Therefore, a well-defined hydrodynamic shape factor is required to replace the surface and projected areas for characterizing the shape-dependent drag coefficient.

Bagheri et al.[21] reported that the contribution of pressure drag and frictional drag to the overall drag of an ellipsoid was strongly dependent on its Aschenbrenner shape factor (ASF = $D_L D_S/D_I$,[2] where D_S is the shortest length of a particle). More specifically, it can be found from the study of Bagheri et al.[21] that, for a sphere (i.e., Aschenbrenner shape factor ASF = 1), one-third of the overall drag is due to pressure drag, and two-thirds is due to frictional drag. Also, with more elongated (ASF > 1) or flatter (ASF < 1) morphologies compared to a sphere,

https://doi.org/10.1021/acs.est.1c06188
Environ. Sci. Technol. XXXX, XXX, XXX−XXX

the contributions of the pressure and friction drags of the particle can be theoretically calculated by using its ASF.[21] Thus, the ASF is a suitable hydrodynamics shape factor.

Moreover, the ellipsoids with elongated and flat morphologies are somewhat similar to fibers or films in morphology, indicating that the Aschenbrenner shape factor is a promising shape factor for distinguishing between fibrous and nonfibrous microplastic particles. As such, the Aschenbrenner shape factor is adopted in this study to explicitly link the morphological and hydrodynamic characteristics of microplastic fibers (to be demonstrated).

2.1.3. Expression of New Drag Model. With the measured terminal settling velocity obtained from the experimental column tests, the Reynolds number ($Re = u_t d_{eq}/\vartheta$) can be determined based on the equivalent diameter of a particle and the kinematic viscosity of the fluid. Also, the measured drag coefficient can be calculated by using eq 4. Subsequently, with the new shape factor (ASF), an explicit expression for the new drag model, which correlates the Reynolds number and the measured drag coefficient, can be derived using regression analysis.[38] The flow-chart of the derivation procedure is illustrated in Supporting Information (SI) Section SI2.

To obtain the explicit expression of the new drag model, a set of comprehensive data is required. Melkebeke et al.[25] reported a data set of column tests for microplastics. The tests included a total of 140 microplastic particles, including fibers, films, and fragments. This data set includes detailed physical properties, such as the density, volume, length scales (i.e., D_L, D_I, D_S, and D_{eqv}), and measured terminal settling velocities for each microplastic particle. As such, the data set reported by Melkebeke et al.[25] is used in this study to develop the new drag model.

It is common practice to use the same data set to develop and evaluate newly proposed models, such as the models proposed by Khatmullina et al.[38] However, this approach may not be ideal and subject to probity. To remedy this problem, we adopt the test/training split method with a 70/30 split ratio[49] that is often used in the field of machine learning. By using this approach, 70% of fiber data reported by Melkebeke et al.[25] is used to obtain an explicit expression of the new drag mode based on nonlinear regression:

$$C_D = \frac{58.58ASF^{0.1936}}{Re^{0.8273}} \tag{6}$$

while the unused 30% of fiber data is used later to evaluate the obtained expression.

2.2. Method of Model Evaluation. *2.2.1. Evaluation of Drag Coefficient.* The drag coefficients calculated by using the measured terminal velocity serve as the important input parameters for developing the new drag model (eq 6). Therefore, the applicability of the expression of the drag coefficient (eq 4) for characterizing microplastic fibers needs to be first evaluated.

Combining the Reynolds number ($Re = u_t d_{eq}/\vartheta$ where ϑ is the kinematic viscosity of the fluid), eq 4 yields

$$C_D Re^2 = \frac{4}{3} Ar^2 \tag{7}$$

where Ar is the Archimedes number:

$$Ar = \sqrt{D_{eqv}^3(\rho_m - \rho_f)g/(\rho_f \vartheta^2)}$$

which is widely used in particle settling problems to quantify the relative importance of the buoyancy force compared to the viscous force acting on a particle. It should be noted that another expression for the Archimedes number, specifically, $Ar' = D_{eqv}^3(\rho_m - \rho_f)g/(\rho_f \vartheta^2 \vartheta 2)$, is also reported in the literature.[50] If the alternative expression for Archimedes number is adopted, eq 4 yields

$$C_D Re^2 = \frac{4}{3} Ar' \tag{8}$$

Since eq 7 and eq 8 have the same physical meaning, eq 7 is adopted in this study.

For a given particle that is settling in a fluid, the particle properties (i.e., V, D_{eqv}, and ρ_m) and fluid properties (i.e., ϑ and ρ_f) are determined such that the Archimedes number of the particle is constant, regardless of the particle morphology. Also, the left side of eq 7 for the given particle is constant and independent of its morphology. Thus, the drag coefficient calculated by any reasonable expression and any equivalent diameter should satisfy eq 7 ($C_D Re^2 = 4Ar^2/3$). It is worthwhile to note that eq 7 has been widely used as a criteria to evaluate the expression of drag coefficient in the fields of environmental science,[11] geological sciences,[51] and industrial processing[52] due to its broad applicability.

To examine the expression of drag coefficient used in this study (i.e., eq 4), the physical properties of fibers and water are first obtained from the data set reported by Melkebeke et al.[25] to calculate the Archimedes numbers (Ar). Also, the drag coefficient (C_D) and Reynolds number (Re) of each fiber are calculated by using different equivalent diameters (i.e., D_L, D_S, and D_{eqv} shown in Table 1, and D_{eqa} calculated with eq 3). Then, $C_D Re^2$ is compared with $4Ar^2/3$ for each fiber to evaluate eq 4.

2.2.2. Evaluation of New Shape Factor. Another important input parameter for developing the new drag model (eq 6), specifically the Aschenbrenner shape factor, is evaluated to assess whether it can be used to differentiate between fibrous and nonfibrous microplastics in terms of morphology. More specifically, the Aschenbrenner shape factor, Corey shape factor, and Dellino shape factor of 140 microplastics in the data set provided by Melkebeke et al.[25] are compared to evaluate their performance on distinguishing different microplastics.

2.2.3. Evaluation of New Drag Model. As discussed, the unused 30% of fiber data reported by Melkebeke et al.[25] is adopted to evaluate the newly proposed drag model (eq 6). Moreover, the new fiber-settling experiments were conducted in this study to produce a unique independent data set for model evaluation. In the experiments, 12 polyester fibers with different sizes were allowed to settle in a column filled with water. The terminal settling velocity of each fiber was measured. Each test was repeated three times. Also, the density, volume, and size of each fiber used in the experiments were measured. The experimental setup, materials, and results are described in SI Section SI1.

It should be noted that the newly proposed drag model (eq 6) is derived based on the volume of a microplastic fiber (cf. eq 4). Although the microplastic volume can be obtained based on the measured mass and density (i.e., $V = M/\rho_m$), existing studies[12,29] generally do not provide sufficient information on the volume of microplastics. Notwithstanding, a robust model should still be able to provide reasonable predictions even if some required input parameters are not well-defined (e.g., fiber volume). Therefore, the data sets from the studies of

https://doi.org/10.1021/acs.est.1c06188
Environ. Sci. Technol. XXXX, XXX, XXX−XXX

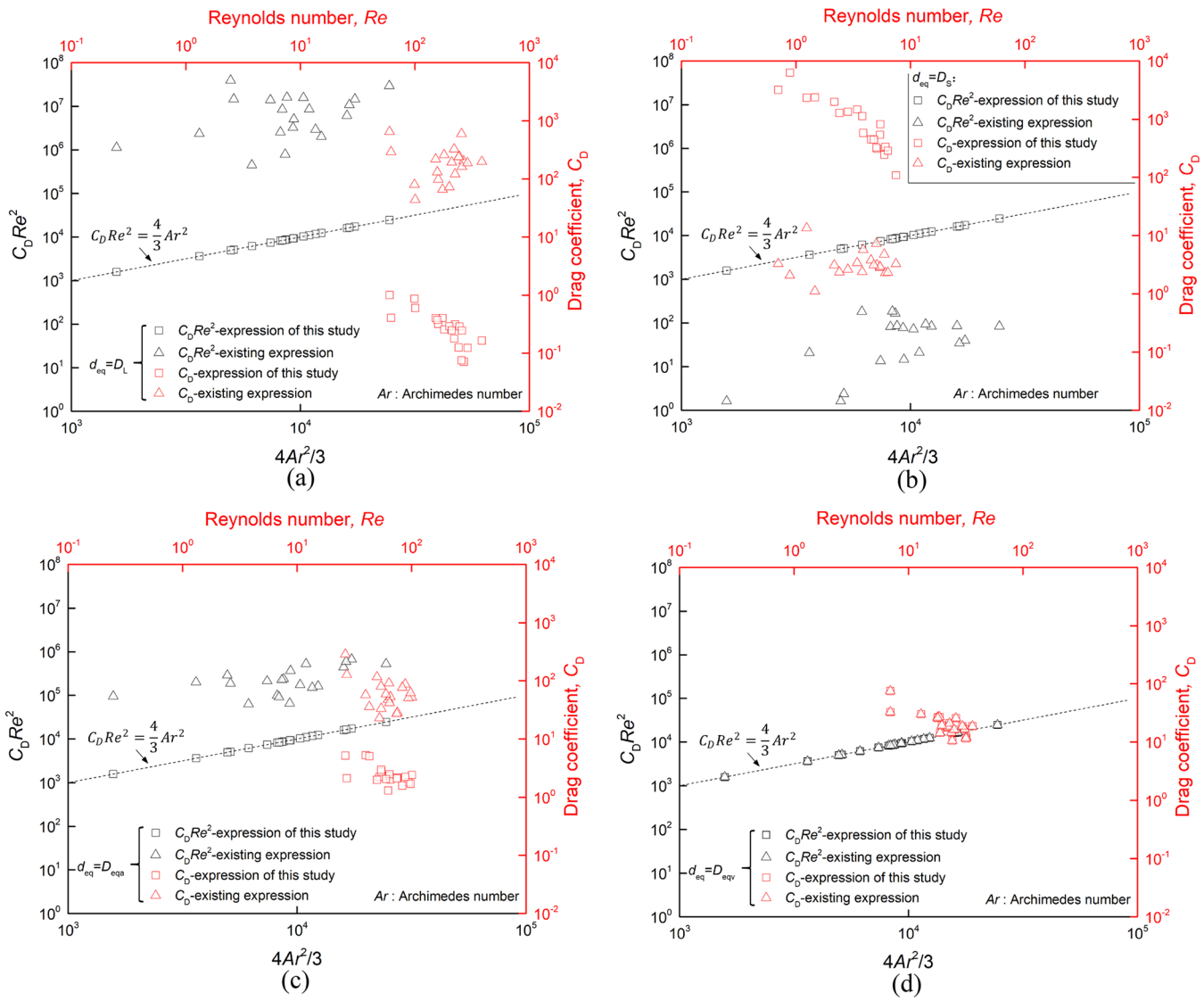

Figure 1. Comparisons of drag coefficients calculated by using the expression proposed in this study (eq 4) and the existing expression (eq 2) with different equivalent diameters. The black dashed line is drawn with $C_D Re^2 = 4Ar^2/3$ (eq 7) to show the theoretical relationship of the drag coefficient, Reynolds number, and Archimedes number. (a) $d_{eq} = D_L$. (b) $d_{eq} = D_S$. (c) $d_{eq} = D_{eqa}$. (e) $d_{eq} = D_{eqv}$..

Waldschlager et al.[12] and Khatmullina et al.,[29] which do not report the fiber volumes, are also used to evaluate the newly proposed drag model (eq 6). The estimated volume (i.e., $V' = D_L D_I D_S$), which has been widely used to calculate the volume equivalent diameter of microplastics,[11,12] is adopted herein to evaluate the newly proposed drag model (eq 6).

Even though the newly proposed model (eq 6) is developed for fibers, it should also be versatile enough to predict the terminal settling velocities of microplastics with other morphologies (e.g., fragments and films). To verify this hypothesis, the data set of microplastic fragments and films reported by Melkebeke et al.[25] is used to evaluate the performance of the newly proposed drag model (eq 6) on predicting the terminal settling velocities of fragments and films.

In addition, to statistically evaluate the performance of a model, the average error (AE) and the coefficient of determination (R^2), which are widely adopted in the literature,[12,38] are used in this study. These two statistic indices are calculated with the measured ($u_{t,mea}$) and calculated ($u_{t,cal}$) terminal settling velocities as follows:

$$\mathrm{AE} = \frac{1}{n}\sum_{i=1}^{n} |(RE)_i| \times 100\% = \frac{1}{n}\sum_{i=1}^{n}\left|\frac{(u_{t,\mathrm{cal}})_i}{(u_{t,\mathrm{mea}})_i} - 1\right| \times 100\% \tag{9}$$

$$R^2 = \frac{\left[\sum(u_{t,\mathrm{mea}}u_{t,\mathrm{cal}}) - \frac{1}{n}\sum u_{t,\mathrm{mea}}\sum u_{t,\mathrm{cal}}\right]^2}{\left[\sum u_{t,\mathrm{mea}}^2 - \frac{1}{n}(\sum u_{t,\mathrm{mea}})^2\right] \times \left[\sum u_{t,\mathrm{cal}}^2 - \frac{1}{n}(\sum u_{t,\mathrm{cal}})^2\right]} \tag{10}$$

where n is the number of individual measurements. The average errors indicate the percentage difference between the calculated and measured velocities. The coefficient of determination is a measure of how well the observed outcomes are described by a particular model. The two statistic indices will be shown along with the evaluation result of each data set adopted in this study.

https://doi.org/10.1021/acs.est.1c06188
Environ. Sci. Technol. XXXX, XXX, XXX−XXX

3. RESULTS AND DISCUSSION

3.1. Evaluation of Expression for Drag Coefficient. Figure 1 shows a comparison of the drag coefficients calculated using different equivalent diameters (i.e., D_L, D_S, D_{eqa}, and D_{eqv}) that are used in existing drag models and this study. Also, the existing expression for drag coefficient (eq 2), which was used in the study of Dioguardi et al.,[29] is compared with the expression for drag coefficient proposed in this study (i.e., eq 4) under different equivalent diameters.

It is observed for a given fiber that the calculated C_DRe^2 using eq 4 is independent of the equivalent diameter, and all calculated values of C_DRe^2 by using eq 4 are equal to $4Ar^2/3$. In contrast, the calculated C_DRe^2 by using eq 2 varies when different equivalent diameters are used. Aside from the volume equivalent diameter (Figure 1d), whereby eq 2 is identical to eq 3, the calculated C_DRe^2 using eq 2 with the other three equivalent diameters are not equal to $4Ar^2/3$. Thus, based on Figure 1, it can be concluded that the modified expression (eq 4) for characterizing the drag coefficient of microplastic fibers is an improvement compared to the existing expression (eq 2). Also, the results indicate that the modified expression (eq 4) has broad applicability.

It should be noted that, for a given fiber, different equivalent diameters in both eq 2 and eq 4 give rise to different calculated drag coefficients. Although eq 7 is used to evaluate drag coefficient expressions (i.e., eqs 2 and 4) based on the relationships among the drag coefficient, Reynolds number, and Archimedes number, eq 7 cannot be used to assess whether a particular equivalent diameter is applicable to fibers. Therefore, the newly proposed drag model (eq 6), including the drag coefficient that is calculated by using the area equivalent diameter, will be further evaluated.

3.2. Evaluation of Aschenbrenner Shape Factor. The morphologies of different microplastic particles reported by Melkebeke et al.[25] are categorized using the indices of elongation ($e = D_I/D_L$) and flatness ($f = D_S/D_I$), which are widely used in the literature.[53] The morphology classification results are presented in SI Section SI3. It can be demonstrated that microplastic fibers are morphologically unique compared to microplastic fragments and films. As discussed, any rational shape factor should be able to be used to distinguish fibers from fragments and films both in morphology and hydrodynamics.[54] Thus, the hydrodynamic shape factor reported by Bagheri et al.,[24] specifically the Aschenbrenner shape factor which is used in the newly proposed drag model (eq 6), is evaluated herein on whether it can distinguish between the different microplastic morphologies. Figure 2 shows a comparison of the performance of two other mainstream shape factors used in existing drag models (i.e., Corey shape factor and Dellino shape factor) with the Aschenbrenner shape factor based on the data set reported by Melkebeke et al.[25]

It can be observed that 88% of the fragments have a Dellino shape factor that is larger than 0.2, and all films and 90% of the fibers have a Dellino shape factor that is between 0.025 and 0.200. This shows that the Dellino shape factor can be used to distinguish between fragments from fibers and films, whereas it cannot be used to clearly differentiate between fibers and films. This is not surprising since the Dellino shape factor originated from geological sciences and was used to describe the shape of pumice,[28] which is fragment-like in morphology and has no morphological resemblance to fibers.

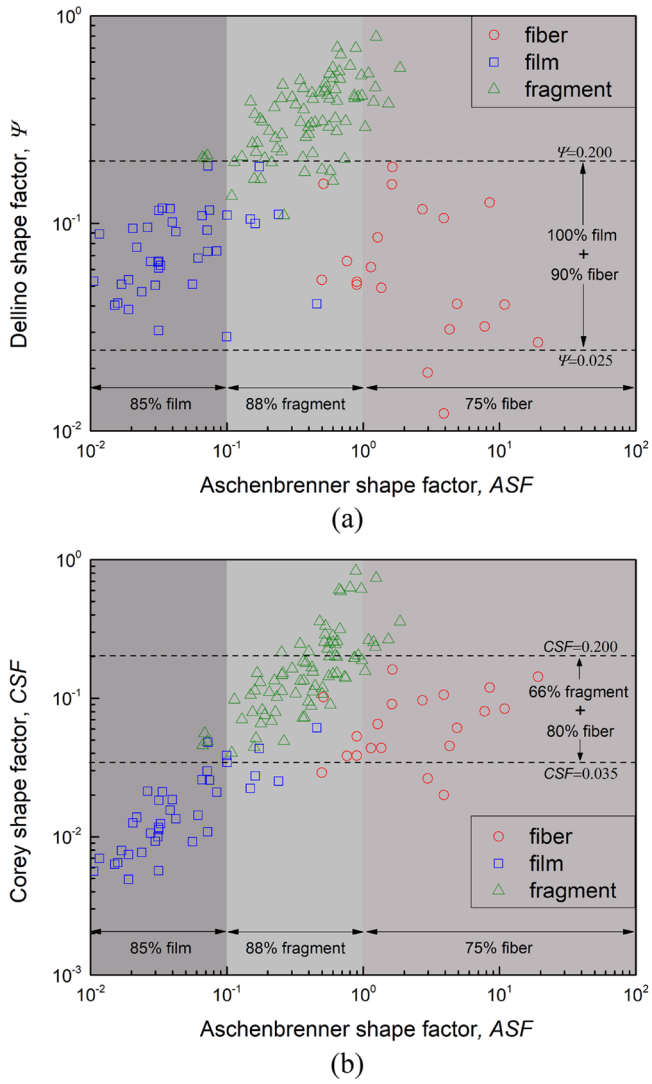

Figure 2. Comparison of Aschenbrenner shape factor and shape factors used in existing drag models on charactersing microplastics in morphology. (a) Comparison of Aschenbrenner shape factor and Dellino shape factor. (b) Comparison of Aschenbrenner shape factor and Corey shape factor.

It is also found that 85% of films have a Corey shape factor that is less than 0.035, whereas all of the fragments and 85% of the fibers have a Corey shape factor that is larger than 0.035. Evidently, the Corey shape factor can be used to distinguish films from fibers and fragments. Nonetheless, the Corey shape factor does not perform well when differentiating fragments from fibers, especially since 80% of fibers and 66% of fragments have a similar range of Corey shape factors, which are between 0.035 and 0.200.

It can be inferred from the aforementioned observations that drag models, which adopt the Dellino shape factor or the Corey shape factor, cannot reasonably predict the terminal settling velocities of fibers since neither of the two factors can clearly characterize the morphology of fibers. In contrast to the Dellino shape factor and the Corey shape factor, 75% of fibers have an Aschenbrenner shape factor that is larger than unity, 88% of fragments have an Aschenbrenner shape factor between 0.1 and unity, and 85% of films have an Aschenbrenner shape factor that is less than 0.1. These observations demonstrate that the Aschenbrenner shape factor can be adopted to provide

https://doi.org/10.1021/acs.est.1c06188
Environ. Sci. Technol. XXXX, XXX, XXX−XXX

an improvement in the characterization of microplastic particle morphologies (i.e., fibers, films, and fragments) compared to the shape factors used in the existing drag models.[12,29]

Moreover, the fiber data sets reported by Khatmullina et al.[38] and the data set of nonfibrous microplastics (e.g., films, pellets, and foams) reported by Waldschlager et al.[55] are used to further evaluate the performance of the Aschenbrenner shape factor. A detailed comparison of the performances of Aschenbrenner shape factor and Corey Shape factor on distinguishing among various microplastic morphologies is available in SI Section SI4. Similarly to the conclusions drawn from Figure 2, the Aschenbrenner shape factor can reasonably distinguish between fibrous and nonfibrous microplastic morphologies.

3.3. Evaluation of Newly Proposed Drag Model.

3.3.1. Prediction of Settling Velocities of Fibers Based on the Measured Fiber Volume. As discussed, the unused 30% of fiber data reported by Melkebeke et al.[25] was used to evaluate the newly proposed drag model (eq 6). Figure 3 shows a comparison of the calculated terminal settling velocities ($u_{t,\mathrm{cal}}$), which are based on different drag models, with the measured ones ($u_{t,\mathrm{mea}}$) reported by Melkebeke et al.[25]

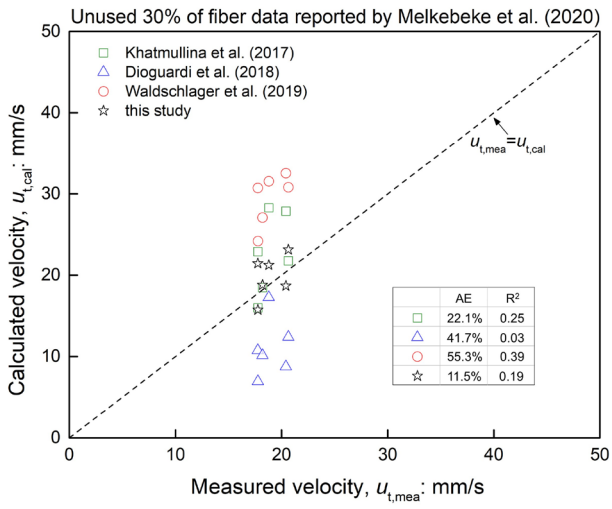

Figure 3. Comparison of calculated and measured terminal settling velocities of fibers for different drag models based on the unused 30% of fiber data reported by Melkebeke et al.[25]

Generally, the calculated velocities using the model proposed by Waldschlager et al.[12] overestimates the terminal settling velocities of the fibers with an average error (AE) of 61.9%. The overestimation is because the Corey shape factor used in their model has been demonstrated to be unable to characterize the morphology of fibers (cf. Figure 2b). Moreover, the model proposed by Dioguardi et al.[29] is observed to underestimate the terminal settling velocities of fibers (AE = 41.7%) since the Dellino shape factor (cf. Figure 2a) used is also not well-suited for characterizing the morphology of fibers. Although the model proposed by Khatmullina et al.[38] exhibits a better performance for predictions of the terminal settling velocities of fibers (AE = 22.1%) compared to the models proposed by Waldschlager et al.[12] and Dioguardi et al.,[29] it still generally overestimates the settling velocities without a shape factor in their model. Compared with the three aforementioned models,[12,29,38] the newly proposed model (eq 6) shows improved agreement with the measured terminal settling velocities for the microplastic fibers (AE = 11.5%). This improved agreement is mainly due to the use of the Aschenbrenner shape factor, which is able to account for the unique morphology of fibers (cf. Figure 2).

The evaluation of the proposed model (eq 6) based on the 30% of unused fiber data reported by Melkebeke et al.[25] is only 6 data points. To ensure that the proposed model is robust, new experiments were carried out to produce a unique set of data for further model evaluation. Figure 4 shows a comparison

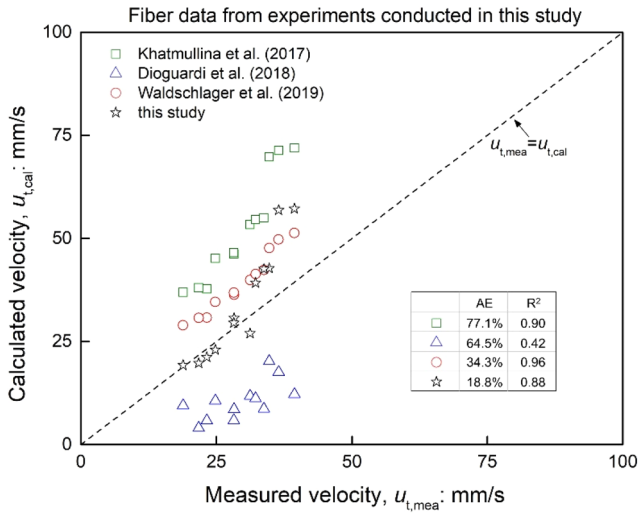

Figure 4. Comparison of calculated and measured terminal settling velocities of fibers for different drag models with the data set from experiments conducted in this study.

of the calculated terminal settling velocities ($u_{t,\mathrm{cal}}$), by using different drag models, with the measured ones ($u_{t,\mathrm{mea}}$) from the new experiment data produced in this study.

It can be observed that the models proposed by Khatmullina et al.[38] and Waldschlager et al.[12] both overestimate the terminal settling velocities of the fibers with average errors of 74.1% and 34.3%, respectively. In contrast, the model proposed by Dioguardi et al.[29] underestimates the settling velocities with an average error of 64.5%. Comparatively, the newly proposed model (eq 6) shows an improved agreement with the measured terminal settling velocities (AE = 18.8%). Thus, combining the evaluation results shown in Figures 3 and 4, it can be demonstrated that the newly proposed model (eq 6) can reasonably predict the terminal settling velocities of microplastic fibers.

3.3.2. Prediction of Settling Velocities of Fibers Based on the Estimated Fiber Volume. It has been demonstrated that, by using the measured fiber volume ($V = M/\rho_{\mathrm{m}}$), the newly proposed drag model (eq 6) reasonably predicts the terminal settling velocities of microplastic fibers. Nonetheless, some studies do not measure or provide measurements of the fiber volume (e.g., Waldschlager et al.[12] and Khatmullina et al.[38]). Thus, the estimated fiber volume, which is calculated by using the fiber size (i.e., $V' = D_{\mathrm{L}}D_{\mathrm{I}}D_{\mathrm{S}}$) has to be adopted herein to further evaluate the newly proposed drag model (eq 6).

First, the data set reported by Waldschlager et al.[12] is used to evaluate the new model (eq 6). Figure 5 compares the calculated terminal settling velocities ($u_{t,\mathrm{cal}}$) by using different drag models with the measured ones ($u_{t,\mathrm{mea}}$).[12]

It can be found that the calculated settling velocities, by using the newly proposed model (eq 6), show reasonable

https://doi.org/10.1021/acs.est.1c06188
Environ. Sci. Technol. XXXX, XXX, XXX−XXX

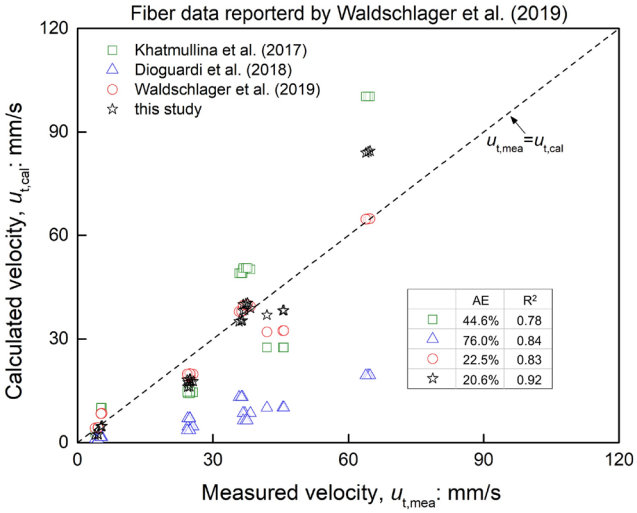

Figure 5. Comparison of the calculated and measured terminal settling velocities of fibers for different drag models by using data set reported by Waldschlager et al.[12]

agreement with the measured terminal settling velocities (AE = 20.6%, R^2 = 0.92). As discussed, the reasonable agreement is attributed to the improvements made by including the Aschenbrenner shape factor, which captures the unique morphology of fibers (cf. Figure 2). This finding suggests that the new model (eq 6) can be used to reasonably predict the terminal settling velocities of microplastic fibers even with an estimated fiber volume.

The model proposed by Waldschlager et al.[12] also reasonably predicts the terminal settling velocities of fibers (AE = 22.5%, R^2 = 0.83). This is not surprising since the model proposed by Waldschlager et al.[12] was developed based on the data set used in Figure 5. Another possible reason for the reasonable predictions of the model proposed by Waldschlager et al.[12] is because of the cylindrical morphology of the fibers used in the study of Waldschlager et al.[12] More specifically, in contrast with the fibers with noncylindrical morphologies (e.g., the fibers used in the study of Melkebeke et al.[25]), both the intermediate length (D_I) and shortest length (D_S) of the fibers with a cylindrical morphology are equal to the fiber diameter (i.e., $D_I = D_S = d$). Thus, the Corey shape factor used in the model proposed by Waldschlager et al.:[12]

$$\mathrm{CSF} = 2D_S/\sqrt{D_L D_I} = \sqrt{d/D_L}$$

includes the same morphological information as the Aschenbrenner shape factor used in the newly proposed model in this study (i.e., ASF = $D_L\, D_S/D_I^2 = D_L/d$). This deduction can also be verified based on a linearly dependent relationship between the Corey shape factor and the Aschenbrenner shape factor for cylindrical fibers (cf. SI Section SI4). Thus, based on the data set reported by Waldschlager et al.,[12] both the model proposed by Waldschlager et al.[12] and the newly proposed model (eq 6) show the reasonable predictions for the settling velocities of fibers.

The model proposed by Dioguardi et al.[29] shows a large average error (AE = 76.0%) because the Dellino shape factor used in this model has been demonstrated to be unable to clearly distinguish fiberous from nonfibrous particles (cf. Figure 2a). Another reason for this large average error is that the Dellino shape factor used in this model needs to be calculated based on the circularity and sphericity (cf. Table 1) of the fibers. Both circularity and sphericity can only be accurately measured by using complex techniques (e.g., 3D scanner or gas adsorption),[24,43] However, in this study, the circularity and sphericity were estimated by using the fiber sizes based on the empirical equation reported by Melkebeke et al.[25] (cf. Table 1). Thus, it is understandable that the model proposed by Dioguardi et al.[29] shows a relatively high average error for the predictions of the terminal settling velocities of fibers. Similarly, the high average error of the model proposed by Dioguardi et al.[29] observed in Figure 4 is also attributed to the estimated circularity and sphericity. It is expected that the prediction accuracy of the model proposed by Dioguardi et al.[29] would be improved if the circularity and sphericity were accurately measured. Nevertheless, it can be found that the model proposed by Dioguardi et al.[29] depends on the accurate measurement to serve as input for complex shape factors. In contrast, the Aschenbrenner shape factor used in the newly proposed model (eq 6) is easy to use and can be obtained based on the fiber size alone (i.e., ASF = $D_L D_S/D_I^2$).

Also, the model proposed by Khatmullina et al.[38] shows a relatively large prediction error (i.e., AE = 44.6%), compared to the newly proposed drag model in this study (eq 6) and the model proposed by Waldschlager et al.[12] This result is not surprising since the model proposed by Khatmullina et al.[38] did not include a shape factor to characterize fiber morphology.

Furthermore, the data set extracted from the study of Khatmullina et al.[38] is used to evaluate the new model (eq 6). Before evaluation, the extracted data was assessed in terms of extraction error. The results show the high reliability of the extracted data, of which the details are described in SI Section SI5. With the extracted data set (204 fiber data points), the calculated terminal settling velocities ($u_{t,cal}$), based on the different drag models, and the measured ones ($u_{t,mea}$)[38] are compared in Figure 6.

Similarly to the evaluation results based on the data set reported by Waldschlager et al.[12] (cf. Figure 5), both the newly proposed drag model (eq 6) and the model proposed by Waldschlager et al.[12] reasonably predict the terminal settling velocities of fibers with average errors of 14.0% and 22.0%,

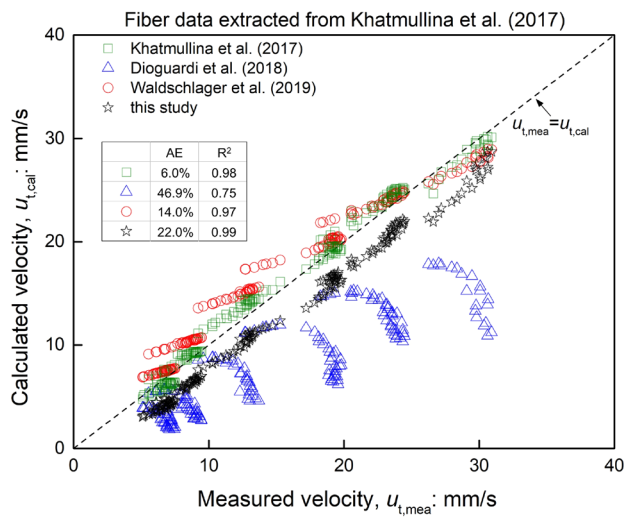

Figure 6. Comparison of calculated and measured terminal settling velocities of fibers for different drag models by using data set extracted from Khatmullina et al.[38]

https://doi.org/10.1021/acs.est.1c06188
Environ. Sci. Technol. XXXX, XXX, XXX−XXX

respectively. This robust performance is as expected since the fibers used by Khatmullina et al.[38] are cylindrical in morphology, which is similar to the fibers used by Waldschlager et al.[12] As discussed, for the fibers with a cylindrical morphology, the Corey shape factor used in the model proposed by Waldschlager et al.[12] includes the same morphological information as the Aschenbrenner shape factor used in the newly proposed model (eq 6). Moreover, based on the evaluation of the performance of the model proposed by Waldschlager et al.[12] and the newly proposed model (eq 6) in Figures 5 and 6, the model proposed by Waldschlager et al.[12] is shown to be able to predict the terminal settling velocities of cylindrical fibers as reasonably as the new model (eq 6), only when its shape factor (i.e., CSF) includes the same morphological information as that of the new model (i.e., ASF). However, for fibers with noncylindrical morphologies (i.e., the fibers used by Melkebeke et al.[25]), the CSF used in the model proposed by Waldschlager et al.[12] is no longer equivalent to the ASF used in the newly proposed model (eq 6). Consequently, as shown in Figure 3, the model proposed by Waldschlager et al.[12] performs noticeably worse compared to the newly proposed model (eq 6) for the fibers with noncylindrical shapes. These results further demonstrate the robustness of adopting the shape factor (ASF) in the newly proposed drag model (eq 6).

The model proposed by Dioguardi et al.[29] exhibits a comparatively large average error (46.9%) since their shape factors (i.e., circularity and sphericity) are estimated by using the fiber sizes instead of being measured. It is worthwhile to point out that, since all of the fiber data shown in Figure 6 has been used to fit the model proposed by Khatmullina et al.,[38] this model naturally exhibits a high accuracy (AE = 6.0%, R^2 = 0.98).

Moreover, the data set provided by the experiments conducted in this study is used to evaluate the applicability of the newly proposed drag model (eq 6) based on the estimated volume (cf. SI Section SI6). Compared with the results calculated by using the measured volume (i.e., AE = 18.8% in Figure 4), the calculated results by using the estimated volume show a higher average error (27.8%). Nonetheless, the new model (eq 6) still performs better than the other three evaluated models (AE = 77.1%, 64.5%, and 34.3%, respectively).[12,29,38] In summary, it can be concluded that, even when the fiber volume is not measured, the newly proposed drag model (eq 6) can still provide reasonable predictions of the settling velocity based on the fiber size.

3.3.3. Prediction of Settling Velocities of Fragments and Films. To verify our hypothesis that the newly proposed drag model (eq 6) can also reasonably predict the terminal settling velocities of microplastics with other morphologies, all of the fragment and film data reported by Melkebeke et al.[25] are used to evaluate the newly proposed model (eq 6). It should be noted that only the 70% of fiber data reported by Melkebeke et al.[25] was used to develop the new model (eq 6), and the remaining fragment and film data was not used to develop the model. Thus, all the fragment and film data reported by Melkebeke et al.[25] can be used to evaluate the newly proposed drag model (eq 6). Figure 7 shows a comparison of the calculated terminal settling velocities ($u_{t,cal}$) for fragments and films by using different drag models with the measured ones ($u_{t,mea}$).

The model that has been identified as the best model for microplastics by Melkebeke et al.[25] is the one proposed by

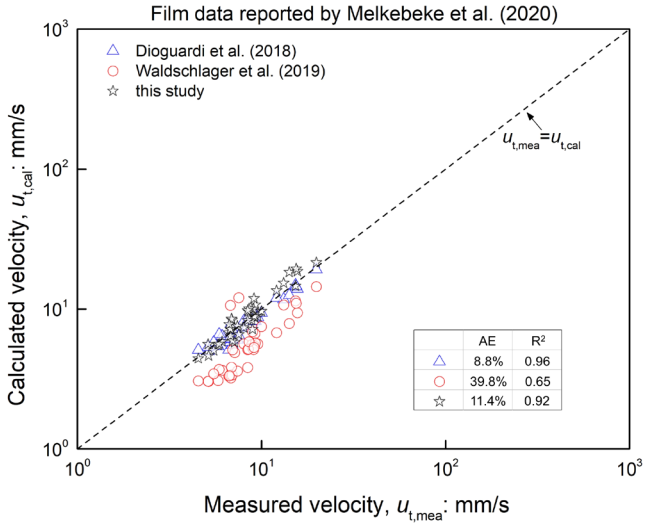

(a)

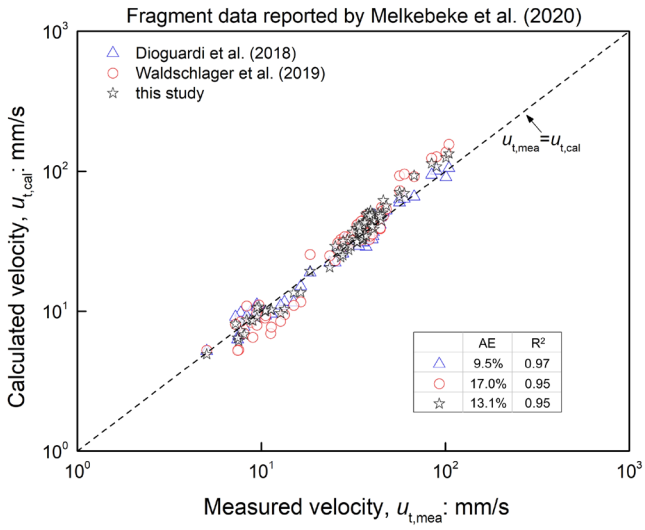

(b)

Figure 7. Comparison of the calculated and measured terminal settling velocities of films and fragments for different drag models by using data set reported by Melkebeke et al.[25] (a) Microplastic films; (b) microplastic fragments.

Dioguardi et al.[26] This model reasonably predicts the terminal settling velocities for both films (AE = 8.8%, R^2 = 0.96) and fragments (AE = 9.5%, R^2 = 0.97). These results should be not surprising since this model was originally proposed for the predictions of the terminal settling velocities of pumice, which are fragment and/or film-like in morphology.

The newly proposed drag model (eq 6) in this study also reasonably predicts the terminal settling velocities of films (AE = 11.4%, R^2 = 0.92) and fragments (AE = 13.1%, R^2 = 0.95). This is because all the parameters used to derive eq 6, specifically the equivalent diameter (eq 3), the expression of the drag coefficient (eq 4), and the Aschenbrenner shape factor, are applicable to microplastic particles with any morphology, including films and fragments.

The model proposed by Waldschlager et al.[12] shows a reasonable performance on predicting the terminal settling velocities of microplastic fragments (AE = 17.0%, R^2 = 0.95). This result is expected because the data of microplastic

https://doi.org/10.1021/acs.est.1c06188
Environ. Sci. Technol. XXXX, XXX, XXX−XXX

fragments had been used when the model was developed.[12] However, this model basically underestimates the terminal settling velocities of microplastic films (AE = 39.8%, R^2 = 0.65). These observed trends are understandable since no data of microplastic films was considered when the models were developed.

3.4. Summary and General Discussion. A new drag model is developed by using the Aschenbrenner shape factor, which can distinguish the morphologies of fibers, films, and fragments. The proposed model is demonstrated to predict the drag coefficient and terminal settling velocity of microplastic fibers more accurately than existing drag models. Also, the new model can reasonably predict the terminal settling velocities of films and fragments.

Despite the improvements made in predicting the terminal settling velocities of micro plastics made in this study. There remain many challenges that have yet to be addressed. More notably, the newly proposed drag model (eq 6) is developed based on the data of virgin microplastic particles reported by Melkebeke et al.[25] Additionally, all of the data, which was used to evaluate the drag models (cf. Figures 3−6), is based on the virgin microplastics in idealized lab conditions. However, it has been reported that weathered microplastics in the field show different settling behaviors compared with the virgin ones.[25] Thus, the applicability of the new model (eq 6) to weathered microplastics remains unclear.

The data set of weathered microplastics reported by Waldschlager et al.[55] is adopted herein to further evaluate the performance of the newly proposed drag model (eq 6) on predicting the terminal settling velocities of weathered microplastics. The comparison between the calculated velocities by using the new model (eq 6) and the measured ones is provided in SI Section SI7. It can be found that the newly proposed drag model (eq 6) based on the virgin microplastics underestimates the settling velocities of the weathered microplastics. Nonetheless, compared with the model proposed by Waldschlager et al.[12] that has been identified as the suitable model for some weathered microplastics (AE = 68.1% and R^2 = 0.73 for films; AE = 46.5% and R^2 = 0.92 for fragments and foams),[44] the newly proposed model (eq 6) shows a comparable performance (AE = 47.7% and R^2 = 0.81 for films; AE = 69.6% and R^2 = 0.82 for fragments and foams). These results are reasonable since the weathering processes in nature generally result in one-sided biofilm growth and nonuniform microplastic densities.[55] However, the virgin microplastics that are used to develop and evaluate the newly proposed drag model (eq 6) are generally uniform in density. Also, another possible explanation for the high prediction errors of these two models for weathered microplastics is that both the Corey shape factors used by Waldschlager et al.[12] and the Aschenbrenner shape factor used by this study cannot distinguish among weathered fragments, foams, and pellets (cf. SI Section SI4). As a result, further research should be undertaken to improve the predictions of the terminal settling velocities of weathered microplastics.

Although the scope of this study mainly focuses on the settling behavior of microplastics, it should be noted that the newly proposed model (eq 6) can also reasonably predict the terminal rising velocities of fibers (cf. SI Section SI8). However, the proposed model is not-well suited for predictions of the rising velocities of nonfibrous microplastics (cf. SI Section SI8). Certainly, the prediction of the rising velocities of nonfibrous microplastics requires more attention in future studies.

■ ASSOCIATED CONTENT

Supporting Information

The Supporting Information is available free of charge at https://pubs.acs.org/doi/10.1021/acs.est.1c06188.

Details of the experiments of microplastic fibers settling in quiescent water (Section SI1); Strategy for developing the new drag model (Section SI2); Morphology characterization of microplastics (Section SI3); Evaluation of Aschenbrenner shape factor with additional data sets (Section SI4); Assessment of extracted data (Section SI5); Evaluation of the new drag model with estimated fiber volume based on the experiment data produced in this study (Section SI6); Applicability of the new drag model to weathered microplastics (Section SI7); Applicability of the new drag model to predictions of terminal rising velocities of virgin microplastics (Section SI8) (PDF)

■ AUTHOR INFORMATION

Corresponding Author

Clarence Edward Choi − *Department of Civil Engineering, The University of Hong Kong, Pok Fu Lam, Hong Kong SAR*; Email: cechoi@hku.hk

Author

Jiaqi Zhang − *Department of Civil Engineering, The University of Hong Kong, Pok Fu Lam, Hong Kong SAR*

Complete contact information is available at: https://pubs.acs.org/10.1021/acs.est.1c06188

Notes

The authors declare no competing financial interest.

■ ACKNOWLEDGMENTS

The author acknowledges the support provided by the Department of Civil Engineering and Faculty of Engineering at the University of Hong Kong for their support provided by the startup fund, and the support from the Research Grants Council of Hong Kong, particularly the funding from the General Research Fund (16212618; 16210219), the Early Career Scheme (27205320), and the Areas of Excellence (AoE/E-603/18).

■ REFERENCES

(1) Xia, W.; Rao, Q.; Deng, X.; Chen, J.; Xie, P. Rainfall is a significant environmental factor of microplastic pollution in inland waters. *Sci. Total Environ.* **2020**, *732*, 139065.

(2) Dibke, C.; Fischer, M.; Scholz-Bottcher, B. M. Microplastic mass concentrations and distribution in German Bight waters by pyrolysis-gas chromatography-mass spectrometry/thermochemolysis reveal potential impact of marine coatings: Do ships leave skid marks? *Environ. Sci. Technol.* **2021**, *55*, 2285−2295.

(3) Suaria, G.; Achtypi, A.; Perold, V.; Lee, J. R.; Pierucci, A.; Bornman, T. G.; Aliani, S.; Ryan, P. G. Microfibers in oceanic surface waters: A global characerization. *Sci. Adv.* **2020**, *6*, 8493.

(4) Hurley, R.; Woodward, J.; Rothwell, J. J. Microplastic contamination of river beds significantly reduced by catchment-wide flooding. *Nat. Geosci.* **2018**, *11*, 251−257.

(5) Cai, Y.; Yang, T.; Mitrano, D. M.; Heuberger, M.; Hufenus, R.; Nowack, B. Systematic study of microplastic fiber release from 12

different polyester textiles during washing. *Environ. Sci. Technol.* **2020**, *54*, 4847−4855.
(6) Garcia, F.; de Carvalho, A. R.; Riem-Galliano, L.; Tudesque, L.; Albignac, M.; Ter Halle, A.; Cucherousset, J. Stable isotope insights into microplastic contamination within freshwater food webs. *Environ. Sci. Technol.* **2021**, *55*, 1024−1035.
(7) Brandon, J. A.; Jone, W.; Ohman, M. D. Multidecadal increase in plastic particles in coastal ocean sediments. *Sci. Adv.* **2019**, *5*, 0587.
(8) Tian, Y.; Chen, Z.; Zhang, J.; Wang, Z.; Zhu, Y.; Wang, P.; Zhang, T.; Pu, J.; Sun, H.; Wang, L. An innovative evaluation method based on polymer mass detection to evaluate the contribution of microfibers from laundry process to municipal wastewater. *J. Hazard. Mater.* **2021**, *407*, 124861.
(9) Zhao, Y.; Qiao, R.; Zhang, S.; Wang, G. Metabolomic profiling reveals the intestinal toxicity of different length of microplastic fibers on zebrafish (Danio rerio). *J. Hazard. Mater.* **2021**, *403*, 123663.
(10) Chubarenko, I.; Bagaev, A.; Zobkov, M.; Esiukova, E. On some physical and dynamical properties of microplastic particles in marine environment. *Mar. Pollut. Bull.* **2016**, *108*, 105−12.
(11) Cowger, W.; Gray, A. B.; Guilinger, J. J.; Fong, B.; Waldschlager, K. Concentration depth profiles of microplastic particles in river flow and implications for surface sampling. *Environ. Sci. Technol.* **2021**, *55*, 6032−6041.
(12) Waldschlager, K.; Schuttrumpf, H. Effects of particle properties on the settling and rise velocities of microplastics in freshwater under laboratory conditions. *Environ. Sci. Technol.* **2019**, *53*, 1958−1966.
(13) Katija, K.; Choy, C. A.; Sherlock, R. E.; Sherman, A. D.; Robison, B. H. From the surface to the seafloor: How giant larvaceans transport microplastics into the deep sea. *Sci. Adv.* **2017**, *3*, No. e1700715.
(14) Pohl, F.; Eggenhuisen, J. T.; Kane, I. A.; Clare, M. A. Transport and burial of microplastics in deep-marine sediments by turbidity currents. *Environ. Sci. Technol.* **2020**, *54*, 4180−4189.
(15) Xue, B.; Zhang, L.; Li, R.; Wang, Y.; Guo, J.; Yu, K.; Wang, S. Underestimated microplastic pollution derived from fishery activities and "hidden" in deep sediment. *Environ. Sci. Technol.* **2020**, *54*, 2210−2217.
(16) Constant, M.; Alary, C.; De Waele, I.; Dumoulin, D.; Breton, N.; Billon, G. To what extent can micro- and macroplastics be trapped in sedimentary particles? A case study investigating dredged sediments. *Environ. Sci. Technol.* **2021**, *55*, 5898−5905.
(17) Waldschlager, K.; Schuttrumpf, H. Erosion behavior of different microplastic particles in comparison to natural sediments. *Environ. Sci. Technol.* **2019**, *53*, 13219−13227.
(18) Rochman, C. M. Microplastics research-from sink to source. *Science* **2018**, *360*, 63−84.
(19) Carr, S. A.; Liu, J.; Tesoro, A. G. Transport and fate of microplastic particles in wastewater treatment plants. *Water Res.* **2016**, *91*, 174−182.
(20) Zhu, X.; Zeng, Y.; Huai, W. Settling velocity of non-spherical hydrochorous seeds. *Adv. Water Resour.* **2017**, *103*, 99−107.
(21) Dietrich, W. E. Settling velcoticy of natural particles. *Water Resour. Res.* **1982**, *18*, 1615−1626.
(22) Camenen, B. Simple and general formular for the settling velocity of particles. *J. Hydraul. Eng.* **2007**, *133*, 229−233.
(23) Song, Z.; Wu, T.; Xu, F.; Li, R. A simple formula for predicting settling velocity of sediment particles. *Water Sci. Eng.* **2008**, *1*, 37−43.
(24) Bagheri, G.; Bonadonna, C. On the drag of freely falling non-spherical particles. *Powder Technol.* **2016**, *301*, 526−544.
(25) Melkebeke, M. V.; Janssen, C.; De Meester, S. Characteristics and sinking behavior of typical microplastics including the potential effect of biofouling: Implications for remediation. *Environ. Sci. Technol.* **2020**, *54*, 8668−8680.
(26) Stokes, G. G. On the Effect of the internal friction of fluids on the motion of pendulum. *Pitt. Press.* **1851**, *9*, 1.
(27) Ahrens, J. P. A fall-belocity equation. *J. Waterway, Port, Coastal, Ocean Eng.* **2000**, *126*, 99−102.
(28) Guo, J. Logarithmic matching and its applications in computational hydraulics and sediment transport. *J. Hydraul. Res.* **2002**, *40*, 555−565.
(29) Dioguardi, F.; Mele, D.; Dellino, P. A new one-equation model of fluid drag for irregularly shaped particles valid over a wide range of Reynolds number. *J. Geophys. Res.: Solid Earth* **2018**, *123*, 144−156.
(30) Haider, A.; Levenspiel, O. Drag coefficient and terminal velocity of spherical and nonspherical particles. *Powder Technol.* **1989**, *58*, 63−70.
(31) Ganser, G. H. A rational approach to drag prediction nonspherical particles. *Powder Technol.* **1993**, *77*, 143−152.
(32) Dellino, P.; Mele, D.; Bonasia, R.; Braia, G.; Volpe, L. L.; Sulpizio, R. The analysis of the influence of pumice shape on its terminal velocity. *Geophys. Res. Lett.* **2005**, *5* (32), L21306.
(33) Dioguardi, F.; Survey, B. G.; Mele, D.; Dellino, P. A new one-equation model of fluid drag for irregularly shaped particles valid over a wide range of Reynolds number: Aerodynamic drag of irregular particles (corrected). *J. Geophys. Res.: Solid Earth* **2018**, *123*, 144−156.
(34) Swamee, P.; Ojha, C. Drag coefficient and fall velocity of nonspherical particles. *J. Hydraul. Eng.* **1991**, *117*, 660−667.
(35) Pfeiffer, T.; Costa, A.; Macedonio, G. A model for the numerical simulation of tephra fall deposits. *J. Volcanol. Geotherm. Res.* **2005**, *140*, 273−294.
(36) Dioguardi, F.; Mele, D. A new shape dependent drag correlation formula for non-spherical rough particles: Experiments and results. *Powder Technol.* **2015**, *277*, 222.
(37) Mandø, M.; Rosendahl, L. On the motion of non-spherical particles at high Reynolds number. *Powder Technol.* **2010**, *202*, 1−13.
(38) Khatmullina, L.; Isachenko, I. Settling velocity of microplastic particles of regular shapes. *Mar. Pollut. Bull.* **2017**, *114*, 871−880.
(39) Kuperman, S.; Sabban, L.; Hout, R. Inertial effects on the dynamics of rigid heavy fibers in isotropic turbulence. *Phys. Rev. Fluids.* **2019**, *4*, 064301.
(40) Marchetti, B.; Raspa, V.; Lindner, A.; Roure, O.; Bergougnoux, L.; Guazzelli, E.; Duprat, C. Deformation of a flexible fiber settling in a quiescent viscous fluid. *Phys. Rev. Fluids.* **2018**, *3*, 104102.
(41) Qi, G.; Nathan, G. J.; Kelso, R. M. PTV measurement of drag coefficient of fibrous particles with large aspect ratio. *Powder Technol.* **2012**, *229*, 261−269.
(42) Yang, X.; Wang, Y.; Yang, H.; Yang, Y. Experimental research on free settling properties of different types of single fiber particle in air. *Build. Environ.* **2020**, *185*, 107300.
(43) Breakey, D. E. S.; Vaezi, G. F.; Masliyah, J. H.; Sanders, R. S. Side-view-only determination of drag coefficient and settling velocity for non-spherical particles. *Powder Technol.* **2018**, *339*, 182−191.
(44) Li, Y.; Gao, S.; Flemming, B. W. Settling velocity and drag coefficient of platy shell fragments. *Sedimentology* **2020**, *67*, 2095−2110.
(45) Toupoint, C.; Ern, P.; Roig, V. Kinematics and wake of freely falling cylinders at moderate Reynolds numbers. *J. Fluid Mech.* **2019**, *866*, 82−111.
(46) Blott, S. J.; Pye, K. Particle shape: A review and new methods of characterization and classification. *Sedimentology* **2007**, *55*, 31−63.
(47) Gogus, M.; Ipekci, N.; Kokpinar, M. A. Effect of particle shape on fall velocity of angular particles. *J. Hydraul. Eng.* **2001**, *127*, 860−869.
(48) Will, J. B.; Mathai, V.; Huisman, S. G.; Lohse, D.; Sun, C.; Krug, D. Kinematics and dynamics of freely rising spheroids at high Reynolds numbers. *J. Fluid Mech.* **2021**, *912*, 912.
(49) Kellenberger, B.; Marcos, D.; Tuia, D. Detecting mammals in UAV images: Best practices to address a substantially imbalanced dataset with deep learning. *Remote Sens. Environ.* **2018**, *216*, 139−153.
(50) Fornari, W.; Picano, F.; Brandt, L. Sedimentation of finite-size spheres in quiescent and turbulent environments. *J. Fluid Mech.* **2016**, *788*, 640−669.
(51) Dioguardi, F.; Mele, D.; Dellino, P.; Dürig, T. The terminal velocity of volcanic particles with shape obtained from 3D X-ray microtomography. *J. Volcanol. Geotherm. Res.* **2017**, *329*, 41−53.

https://doi.org/10.1021/acs.est.1c06188
Environ. Sci. Technol. XXXX, XXX, XXX−XXX

(52) Gabitto, J.; Tsouris, C. Drag coefficient and settling velocity for particles of cylindrical shape. *Powder Technol.* **2008**, *183*, 314−322.
(53) Luo, J.; Xu, Z.; Ren, Z.; Wang, K.; Yang, K.; Tang, Y.; Gao, H.; Tian, L. Rock avalanche-debris geometry and implications for rock-avalanche genesis. *Geomorphology* **2019**, *334*, 60−75.
(54) LE Roux, J. P. Comparision of sphericity indices as related to the hydraulic equivalence of settling grains. *J. Sediment. Res.* **1997**, *3*, 527−530.
(55) Waldschlager, K.; Born, M.; Cowger, W.; Gray, A.; Schuttrumpf, H. Settling and rising velocities of environmentally weathered micro- and macroplastic particles. *Environ. Res.* **2020**, *191*, 110192.

https://doi.org/10.1021/acs.est.1c06188
Environ. Sci. Technol. XXXX, XXX, XXX−XXX